

Titania nanoengineering towards efficient plasmonic photocatalysis: Mono- and bi-metal-modified mesoporous microballs built of faceted anatase



Zhishun Wei^a, Limeng Wu^a, Xin Yue^a, Haoran Mu^b, Zhenhao Li^a, Ying Chang^{a,**}, Marcin Janczarek^c, Saulius Juodkazis^b, Ewa Kowalska^{d,e,*}

^a Hubei Provincial Key Laboratory of Green Materials for Light Industry, Hubei University of Technology, Wuhan 430068, PR China

^b Swinburne's Centre for Micro-Photonics, Swinburne University of Technology, John St, Hawthorn, VIC 3122, Australia

^c Institute of Chemical Technology and Engineering, Poznan University of Technology, Berdychowo 4, 60–965 Poznan, Poland

^d Faculty of Chemistry, Jagiellonian University, 03–387 Krakow, Poland

^e Institute for Catalysis, Hokkaido University, 001–0021 Sapporo, Japan

ARTICLE INFO

Keywords:

Titania microballs

Faceted anatase

CO₂ reduction

H₂ generation

Plasmonic photocatalysis

ABSTRACT

Preparation of porous micro-sized materials with solar response is urgent for fast commercialization of green technologies based on semiconductor photocatalysis. Here, mesoporous titania microballs composed of nanocrystalline anatase with exposed facets were prepared by a sub-zero sol-gel method followed by hydrothermal/alcothermal crystallization. The mechanism of microballs formation and the influence of preparation conditions on the properties, and thus resultant photocatalytic activity, were investigated in detail. The photocatalytic performance was examined in four reaction systems under UV/vis irradiation, i.e., oxidative decomposition of methyl orange (MO) dye, hydrogen evolution, degradation of tetracycline (TC) antibiotic, and carbon dioxide reduction. Moreover, hydrogen generation was also examined under visible-light (vis) irradiation. Amorphous and faceted (octahedral- and decahedral-based) microballs were additionally modified with nanoparticles (NPs) of noble metals (Pt, Au, Ag, Pt/Au, Pt/Ag) for both UV-activity enhancement and vis response (i.e., plasmonic photocatalysis). It has been found that nano-architecture of microballs might be controlled by the ratio of alcohol to water used during hydrothermal/alcothermal treatment. Accordingly, highly active microballs composed of pure octahedral- or decahedral-shaped anatase crystals, i.e., with {101} facets only (bipyramids) or eight {101} and two {001} facets, respectively, could be synthesized by a facile and environmental-friendly method. The versatility and high activity of faceted microballs have been confirmed in both oxidation and reduction reactions under UV and/or vis irradiation (comparable performance to that by famous P25). Decahedral-based samples exhibit usually higher photocatalytic activity than octahedral ones, despite worse photoelectronic properties (charge carriers' separation, electron transport capacity and photocurrent density), due to higher hydrophilicity. However, single type {101} facet photocatalyst (octahedral shape) is preferable for efficient CO₂ adsorption and reduction into CO and CH₄. Among noble metals, though platinum shows much higher positive effect on UV activity, gold is responsible for the highest activity under vis, which corresponds to the strongest plasmonic field enhancement, as proven by finite difference time domain (FDTD) simulations. Concluding, micro-sized balls composed of faceted anatase are undoubtedly prospective photocatalyst for diverse environmental applications.

1. Introduction

Mesoporous materials, i.e., the porous structures of 2–50-nm pores, offer unique properties, such as high specific surface area, large pore

volume, convex surface, patterned arrangement of surface functionalities and synthesis-controlled properties (composition, crystallinity, specific surface area, morphology, structure, topology and pore size), which makes them highly interesting for applications in catalysis,

* Corresponding author at: Faculty of Chemistry, Jagiellonian University, 03–387 Krakow, Poland

** Corresponding author.

E-mail addresses: cy0025@hbut.edu.cn (Y. Chang), kowalska@cat.hokudai.ac.jp, ewa.k.kowalska@uj.edu.pl (E. Kowalska).

photocatalysis, and electrochemistry, as well as for energy purposes (conversion and storage) [1,2]. For example, mesoporous titania (titanium(IV) oxide; TiO_2) spheres composed of nanosized crystallites have recently been intensively investigated for heterogeneous photocatalysis [3,4], dye-sensitized solar cells (DSSCs) [5], lithium-ion batteries [6], and electrochromic displays [7]. Especially, micrometer-sized mesoporous spheres have attracted much attention for photocatalytic application due to high light-harvesting efficiency and facile recovery after reaction [8,9]. Additionally, the porous structure of titania mesoporous spheres allows efficient adsorption of oxygen, water and other reactants, and thus resulting in high photocatalytic activity.

Titania, the most widely investigated semiconductor photocatalyst, might exist naturally in crystalline (e.g., anatase, rutile, brookite and bronze-type) and amorphous forms, as well as a mixture of different phases (most common). It is well known that usually anatase shows the highest photocatalytic activity, because of low recombination rate of photo-generated charge carriers (electrons and holes), probably due to high mobility of electrons, resulting from the low content of deep electron traps [10–12]. Importantly, anatase crystals with faceted morphology, i.e., with exposed {101} facets and exposed high-energy {001} facets, show exceptionally high photocatalytic activity [13,14], because of preferential transfer of photogenerated electrons via shallow electron traps [15], and efficient separation of charge carriers, resulting from selective migration of electrons and holes to {101} and {001} facets, respectively [16–18].

Therefore, mesoporous titania microballs composed of faceted anatase particles, and thus with hybrid properties, such as high specific surface area, high pore volume, controlled pore size, microspherical structure, and efficient separation of charge carriers, should appear as a superior candidate for the use in various photoelectrochemical applications, especially those in which the diffusion of photons and molecules through the pore structure is vital for optimal performance, and a highly ramified network of mesopores is desired [19].

The hollow titania spheres composed of anatase crystals with exposed {001} facets have already been prepared via a fluoride-mediated self-transformation route [20,21]. However, the resulting crystals are too large to obtain a suitable pore structure and high specific surface area, and thus the practical applicability of these spheres is limited. Accordingly, the preparation of mesoporous spheres/balls consisting of titania nanocrystals with exposed high energy facets remains still a challenge [22]. Herein, mesoporous titania microballs composed of amorphous titania nanoparticles (NPs) have been prepared via a sub-zero sol–gel process, and employed as the precursor for the fabrication of faceted-anatase-based mesoporous microballs, i.e., with exposed low-energy {010} and/or high-energy {001} facets, via hydrothermal/alcohothal treatment. Importantly, the morphology, monodispersity, and microball diameter might be controlled via a cooperative self-assembly process in the sub-zero sol–gel synthesis, whereas the crystallite size, specific surface area, and pore size distribution might be tuned by heat treatment during hydrothermal/alcohothal process. The impact of synthesis conditions (e.g., ethylene glycol bath temperature, static time, temperature of thermal treatment and alcohol/water ratio) on morphology, microballs' monodispersity, crystal phase and crystallinity during the synthesis is discussed in detail. Moreover, for efficient light harvesting, microspheres have been mono- and bi-modified with NPs of noble metals (Pt, Ag, Au, Pt/Au and Pt/Ag). Finally, plasmon resonance feature has also been modeled by FDTD simulations for understanding the photocatalytic performance under visible-light (vis) irradiation.

2. Experimental details

2.1. Preparation of mesoporous titania microballs (amorphous structure)

Mesoporous titania microballs were prepared by a sol–gel process. All reagents, i.e., absolute ethanol (AR Sinopharm), tetrabutyl titanate

(TBOT, AR Macklin) and potassium chloride (KCl, AR Sinopharm), were reagent-grade, and thus used without further purification. Deionized water (18.2 MΩ cm) was used in all experiments. In brief, 0.5 mL KCl aqueous solution (0.05 mol/L) was mixed with 100 mL absolute ethanol in a 200-mL round-bottomed flask, which was placed in an ethylene glycol bath with precisely controlled temperature (between 10 and -30 °C) using a low-temperature cryotrapping instrument. Then, 4 mL TBOT was rapidly added into the flask under continuous stirring. After capping the neck of the flask with a septum, the mixture was further stirred for 5 min, and then aged in a static condition for 5 h at three different temperatures, i.e., -10 °C, 0 °C and ca. 25 °C (room temperature). The powders, collected from the bottom of the flask, were washed (four times with ethanol and then four times with deionized water), centrifuged and finally freeze dried (Freezone 6, Labconco). The obtained samples were named as S1, S2, and S3, respectively. Additionally, the influence of aging duration (at -10 °C) has been investigated, and thus five different static times have been examined, i.e., 1, 2.5, 5 (S1 sample), 10 and 20 h.

2.2. Fabrication of crystalline mesoporous microballs

The amorphous titania microballs (sample S1) were used as a precursor to fabricate the mesoporous microballs composed of anatase with exposed facets. The detailed fabrication procedure was as follows: 0.2 g of sample S1 was added to a beaker containing 20 mL liquid (pure deionized water, pure ethanol or deionized water-ethanol mixtures) and kept under stirring for 2 h to get a uniform suspension. Subsequently, the suspension was transferred into a 100-mL Teflon-lined autoclave, and hydrothermal/alcohothal treatment was carried out at 200 °C for 48 h with different volume (mL) ratio of ethanol to water (i.e., 60:0, 58:2, 56:4, 54:6, 52:8, 50:10, 0:60). After hydrothermal/alcohothal treatment, the white precipitates were collected, washed with distilled water and alcohol four times each, centrifuged and dried in a vacuum oven at 80 °C.

2.3. Modification of crystalline mesoporous microballs with noble metals

Two kinds of crystalline mesoporous microballs (octahedral and decahedral) were modified with 2 wt% of noble metal (NM: Pt, Au, Ag, Pt/Au, Pt/Ag) by photodeposition. In brief, the respective salt ($\text{H}_2\text{PtCl}_6 \bullet 6 \text{ H}_2\text{O}$, $\text{HAuCl}_4 \bullet 3 \text{ H}_2\text{O}$ and AgNO_3) was dissolved in an aqueous solution of methanol (50 vol%), bubbled with argon (to remove oxygen), and then, irradiated with mercury lamp for 60 min. The obtained NM-modified titania was washed with methanol and water (three times each), centrifuged and vacuum dried at 60 °C for 12 h. For clarity, obtained samples were named respectively to the deposited metal and the type of microballs, where Pre, Octa and Deca state for precursor (S1 sample), octahedral-shaped (pure ethanol; 60:0 sample) and decahedral-shaped (56:4 sample) microballs, respectively.

2.4. Characterization

The morphology of microballs was investigated by field-emission scanning electron microscopy (FE-SEM, Hitachi SU8010). The crystalline properties of the powders were examined by X-ray diffraction (XRD) using a PANalytical's X'Pert PRO diffractometer ($\text{Cu K}\alpha$ radiation, 40 kV, 40 mA) with 2θ scan range of 10–90° at a rate of 2°/min. The average crystallite size of anatase was estimated using the X'Pert HighScore computer program combined with the Scherrer formula, where the instrumental line broadening was corrected with a silicon standard. The specific surface area and the distribution of pore sizes were estimated by N_2 adsorption measurements, performed on a Micromeritics ASAP 2020 apparatus at 77 K, using the multiple-point Brunauer–Emmett–Teller (BET) theory (the relative pressure range: $P/P_0 = 0.05–0.3$) and the Barrett–Joyner–Halenda (BJH) model, respectively. The photocatalytic activity was evaluated for four model reactions under UV-vis

irradiation, i.e., (i) oxidative decomposition of methyl orange (MO) dye, (ii) water reduction, (iii) oxidative decomposition of tetracycline hydrochloride (TC) antibiotic, and (iv) carbon dioxide reduction. In brief, for (i) MO degradation, an aqueous solution of MO (100 mL, 20 mg/L) was added to 100 mg of photocatalyst placed in a 250-mL testing glass container. The adsorption-desorption equilibrium was obtained during 0.5-h stirring in the dark, then the tube was irradiated with a high-pressure Xe lamp (300 W). The changes in MO concentration were estimated from the absorption spectra measured on a UV-vis-NIR spectrophotometer (UV-1800) after photocatalyst separation via centrifugation (GL-20 G-C).

The photocatalytic performance during hydrogen generation (ii) was evaluated at 25 °C in a closed glass reaction system, which was all-glass automatic on-line trace gas analysis system (Labsolar-6A) from Beijing Perfectlight Technology Co., Ltd. The photocatalyst (0.05 g) was uniformly dispersed by ultrasounds in an aqueous solution (100 mL) containing triethanolamine (TEOA, 10 vol%) as a sacrificial electron donor. The reactor was evacuated with a vacuum pump, and then the content was irradiated with 300-W xenon lamp. For visible-light activity testing, 420-nm cut-off filter was mounted in the front of the lamp. The temperature of the reaction suspension was maintained at 5 °C by circulating cooling water during the photocatalytic experiment. The concentration of generated hydrogen was estimated by on-line gas chromatography system (GC9790II), equipped with a highly sensitive thermal conductivity detector (TCD), using Ar as a carrier gas. Since bare titania is practically inactive for hydrogen evolution reaction, 2 wt % of noble metal (Pt, Au, Ag, Pt/Au and Pt/Ag; 4 wt% in total in the case of bimetallic samples) was deposited on the surface of microspheres by photodeposition using 1-h UV irradiation (Hg lamp).

In the case of TC degradation (iii), 30 mg of sample was suspended in 100 mL of TC solution (25 mg/L) under stirring. The suspension was first kept under stirring in the dark for 0.5 h to reach an equilibrium of adsorption-desorption, and then irradiated for 1 h under UV/vis irradiation (300-W Xe lamp). The reaction temperature was maintained at 25 °C with circulating cooling water. At regular intervals of 15 min, 4-mL samples were withdrawn, centrifuged (to remove the photocatalyst powder) at 4500 rpm for 5 min, and then supernatant was analyzed with UV-Vis spectrophotometer (at 357 nm). Additionally, scavenger tests were carried out to examine the mechanism of TC degradation. Four reagents (0.2 mM), i.e., p-benzoquinone (BQ), isopropanol (IPA), disodium ethylenediaminetetraacetic acid (EDTA-2Na), and silver nitrate (AgNO_3), were used to scavenge superoxide radicals (O_2^-), hydroxyl radicals (OH^{\bullet}), holes (h^+) and electrons (e^-), respectively. The scavengers were added to the suspension containing TC (25 mg/L) and titania microballs (30 mg).

Finally, the carbon dioxide reduction (iv) was also examined. The photoactivity tests were performed in the same reactor, which was used for water reduction (ii). The photocatalyst (0.05 g) was uniformly dispersed in an aqueous solution (27 mL) containing 10 mL of triethanolamine (TEOA, 10 vol%) and 63 mL of acetonitrile. CO_2 was bubbled into the liquid phase containing a photocatalyst. The generated gases (CO , CH_4 , C_2H_4 , C_2H_6 , H_2) were determined by on-line gas chromatography system (GC9790II) equipped with the highly sensitive flame ionization detector (FID).

For visible-light activity testing, the reaction (ii) was performed under vis irradiation, i.e., 300-W Xe lamp with cut-off filter ($\lambda > 420$ nm).

Numerical simulation of localized light enhancement was modeled by finite difference time domain (FDTD) calculations (Lumerical, Ansys). Micrometer-sized titania micro-spheres with nano-spheres of Au, Pt, Ag were illuminated using total-field scattered-field (TFSF) light source, which allowed to calculate cross-sections of scattering and absorption (extinction coefficient is their sum). The material properties were taken from Lumerical database.

3. Results and discussion

3.1. The impact of preparation conditions on the properties of amorphous microballs

The mesoporous microballs have been successfully prepared, as evidenced by microscopic observations (Fig. 1). The morphology of S1, S2 and S3 samples, i.e., prepared at three different temperatures of -10 °C, 0 °C and 25 °C, respectively, resembles dandelion seedhead. Importantly, 0.3–2 μm microballs have not been aggregated, i.e., only single balls exist in the product. It has been found that the reaction temperature is crucial for the nucleation and the growth of NPs, influencing the microballs' topology/morphology. Both the mesoporosity and the particle size have decreased with an increase in the reaction temperature. The high-magnification image of sample S1 (Fig. 1b) reveals that microballs possess a 3D-interconnected-mesoporous framework (of relatively rough surface), built of tiny NPs of 10–20 nm. Indeed, the mesoporous nature has been confirmed by N_2 adsorption-desorption isotherms, as shown in Fig. 2. The typical hysteresis loop at relative pressure range of 0.48–1.0 confirms the presence of mesopores (1–20 nm) [23,24]. Upon a temperature increase, the rates of nucleation and growth are intensified, leading to a decrease in the sizes of microballs and NPs composing them (Fig. 1(c-d)). Accordingly, the adsorption isotherms shift downward (Fig. 2), as clearly observed by the difference in isotherms between sample S1 and those prepared at lower temperatures, indicating still mesoporous nature, but lower pore volume.

Furthermore, the effect of aging duration has been investigated at -10 °C, and exemplary SEM images of the obtained samples are shown in Fig. 3. It has been found that the extension of static time (from 1 h to 20 h) results in an increase in the microballs' diameter and their uniformity (disappearance of the smallest microballs), as well as the smoothing of their surface (Fig. 3(d-e)). It is thought that extended aging time might diminish the mesopores between primary NPs via Ostwald ripening – The dissolved particles might re-deposit onto other pre-existing particles, which results in the pore plugging and smoothing of the microballs surface. Considering the highest uniformity and mesoporous nature, the sample prepared during 5-h aging (S1) has been selected for the further study.

3.2. Preparation of mesoporous microballs composed of faceted anatase NPs

It is well known that amorphous materials are characterized by large content of defects, and thus the low level of photocatalytic activity [25, 26]. Accordingly, amorphous titania (sample S1) has been crystallized via hydrothermal/alcohotermal treatment, i.e., at 200 °C for 48 h with different volume (mL) ratios of ethanol to water (i.e., 60:0, 58:2, 56:4, 54:6, 0:60), and the morphology of the obtained products is shown in Fig. 4. Fortunately, post-treatment has not changed the spherical shape of microballs, as clearly shown in the insets of Fig. 4. The products are characterized by hierarchical structure with pore networks and 1–2- μm size. Interestingly, magnified images (main pictures in Fig. 4) indicate that microballs are composed of well-ordered NPs, suggesting their high crystallinity. Indeed, clear diffraction peaks of anatase phase could be observed in Fig. 5 for all post-treated samples. In contrast, there is not any peak in the case of S1 sample (precursor), confirming its amorphous nature. It should be pointed out that usually the phase transformation from amorphous titania into anatase crystals occurs at much higher temperatures (above 300 °C; under atmospheric pressure in an oven). Hence, it might be concluded that hydrothermal/alcohotermal treatment enhances the phase transformation of titania at low temperature due to non-equilibrium-pressure conditions. The crystallite sizes, estimated by Scherrer formula (Table S1) [27,28], correlate well with NPs' sizes, observed by high-magnification FE-SEM (Fig. 4).

The most crucial finding of this study is the formation of facet-shaped anatase NPs, as clearly seen in Fig. 4. It should be pointed out that

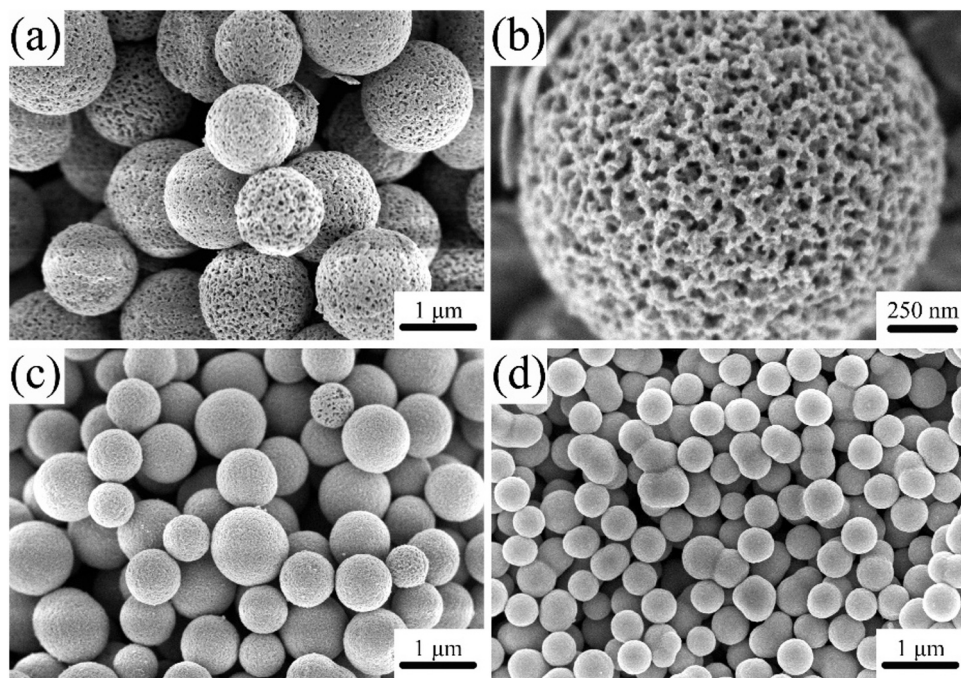


Fig. 1. FE-SEM images of microballs synthesized at (a-b) -10 °C (sample S1), (c) 0 °C (sample S2), and (d) room temperature (25 °C, sample S3).

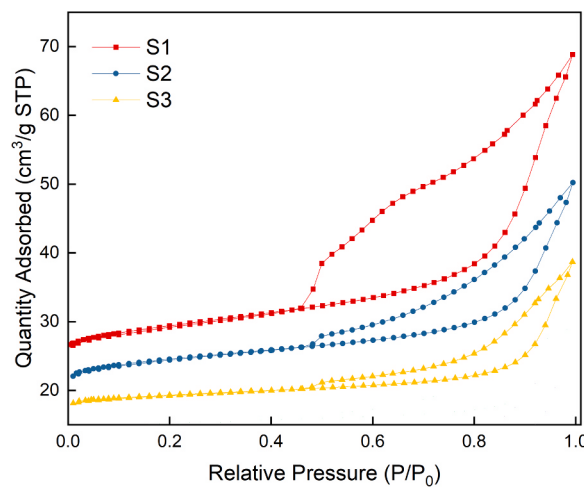


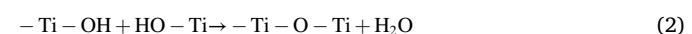
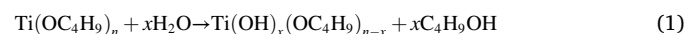
Fig. 2. Nitrogen-adsorption-desorption isotherms of S1, S2 and S3 samples.

usually the synthesis of titania with controlled morphology is challenging, involving many reaction steps, and often the morphology-control agents must be used [29–33]. Here, just simple post-treatment operation results in the preparation of microballs built of faceted anatase NPs. For example, the sample synthesized by alcothermal treatment in pure alcohol (ethanol/water ratio of 60:0) exhibits a perfect octahedral structure with dominant {101} facets (Fig. 4a), whereas coexistence of octahedron and decahedron is observed in the sample prepared by hydrothermal treatment, i.e., in pure water (ethanol/water ratio of 0:60). Accordingly, it is thought that alcohol might act as a protecting agent, inhibiting the formation of {001} facets. Therefore, the selective coordination of {001} surfaces retards the crystal growth along the [001] direction [25,26], and thus ensuring the preferential growth of {101} facets. With an addition of water, the decahedron shape appears, i.e., anatase with eight equivalent {101} facets and two equivalent {001} facets (Fig. 4b). The further reduction of the ethanol/water ratio to 56:4 results in the formation of sheet-like decahedron with the side length of ~80 nm and the thickness of ~40 nm (Fig. 4c), whereas the

54:6 ratio causes the generation of mainly decahedral nanocrystals with sharp edges, and notably, well developed {101} and {001} facets (Fig. 4d). The calculated ratio of exposed {001} facets in dependence on the ratio of ethanol to water is shown in Fig. S1.

3.3. Mechanism of faceted NPs formation

It is known that massive precipitation of amorphous titania occurs inevitably in most sol-gel preparation methods, due to very fast hydrolysis and condensation, and hence the uncontrolled branching of the resulting Ti-O-Ti network. Herein, monodisperse microballs (precursor) with wormhole-like mesoporous structure have been formed through a slow precipitation of titania particles from titania alkoxides in an aqueous alcohol solution, involving an interplay of electrostatic, van der Waals, and short-range repulsive interactions [27]. During hydrolysis of TBOT, a clear solution turns first into a slightly blue colloidal one, where the reaction between TBOT and H₂O results in coordination of water to titanium centers, forming unstable titanium complexes $Ti(OH)_x(OC_4H_9)_{n-x}$ by ligand exchange/substitution, concomitant with a release of C₄H₉OH (Eq. 1). Subsequently, Ti-O-Ti bonds are formed by both hydrolysis-condensation and nonhydrolytic condensation processes (Eqs. 2 and 3). When the phase separation (condensation) happens gradually with time, undirectional aggregation causes the formation of amorphous spherical particles as a result of minimization of surface free energy [28], which leads to the formation of milky white suspension [29]. Considering the induction time (the period after addition of TBOT until the milky white suspension is formed) and hydrolysis temperature (the static condition at -10 °C, 0 °C and 25 °C), the formation of monodisperse mesostructured microballs correlates closely to the proposed mechanism, as shown in Fig. 6. It is noteworthy that the wormhole-like mesoporous microballs disappear (being smoother) with an increase in hydrolysis temperature or an extension of induction time (Fig. 3(e)), which should be caused by a cementation mechanism inside the aggregates [27].



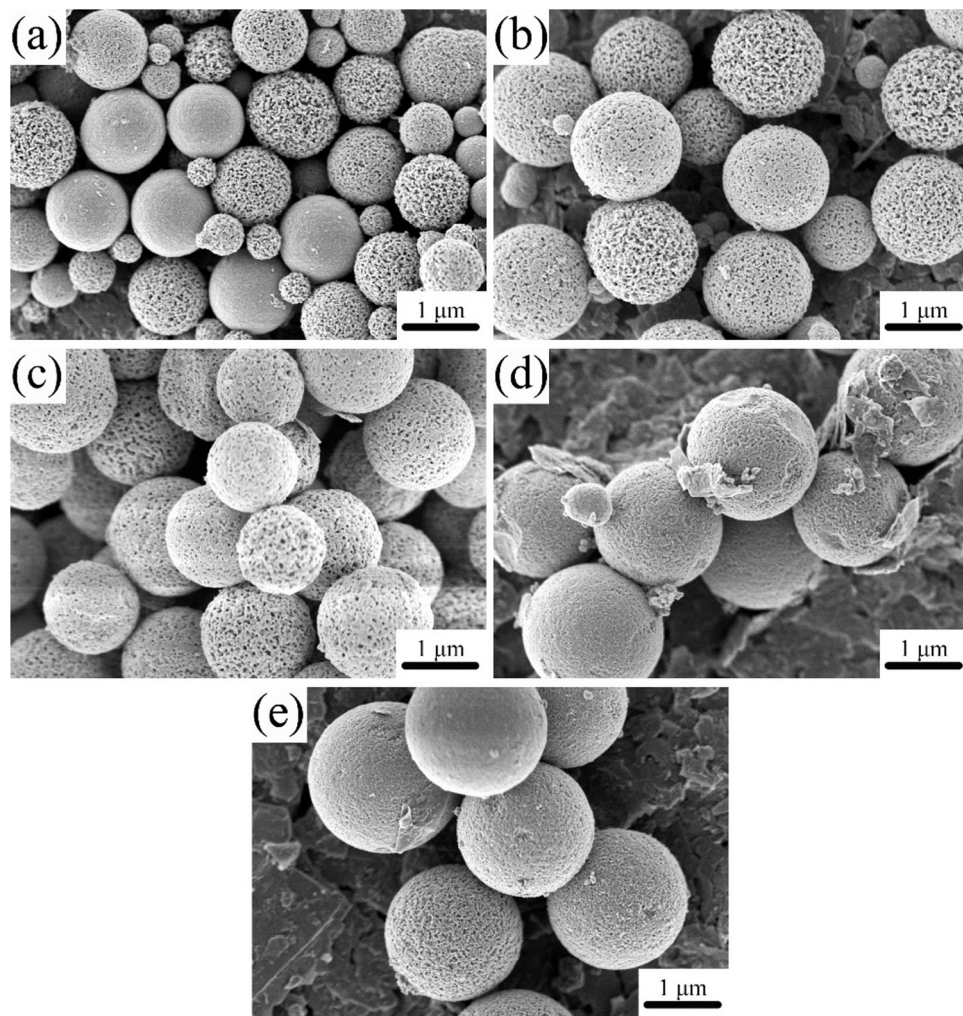
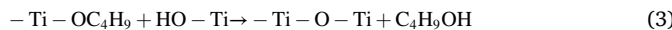


Fig. 3. FESEM images of amorphous titania microballs synthesized at $-10\text{ }^{\circ}\text{C}$ for (a) 1 h, (b) 2.5 h, (c) 5 h, (d) 10 h, and (e) 20 h of static time.



On the basis of the preparation of amorphous microballs with wormhole-like mesoporous structure (precursor), the hydrothermal/alcohotermal process has been chosen to obtain crystalline microballs with high-energy exposed facets, such as {001} and {100}/{010}, and low-energy {101} facets [30]. A mechanism for the formation of monodisperse anatase microballs has been proposed to illustrate the role of water/alcohol during the synthesis. Considering the effect of water/alcohol on enhanced crystallization of amorphous titania [31], the incompletely hydrolyzed precursor undergoes a further in situ hydrolysis and condensation at the interface between particles and hot water/alcohol, then fine anatase nanocrystals are formed due to the lower surface energy than other phases [32]. Because of the presence of wormhole-like mesoporous structure, hot water/alcohol might also penetrate into the interior of the precursor microballs to carry on the above-mentioned Ostwald ripening process [33], i.e., the smaller crystals slowly disappear acting as “nutrients” for the growth of larger ones, while the larger crystallites serve as starting points (nucleation seeds) on the outermost surface of microballs. Since hydrothermal/alcohotermal reaction involves a dissolution-redeposition procedure, the surface becomes rough, as shown in Fig. 4. Finally, anatase mesoporous microballs are obtained.

To further explore the exposed facets formation, the process has been controlled by varying the ratio of alcohol to water, keeping other parameters, such as the reaction temperature, the reaction duration, the

type of alcohol and the total volume of liquid phase, fixed. It is known that morphology evolution of a crystal in gas or liquid phases is determined by the driving force of the further reduction in energy, due to the minimization of the area of high-surface-energy facets (the thermodynamics point of view), whereas the crystal morphology is defined by the slowest growing facets because the fastest growing ones shrink (the kinetics point of view) [34]. Herein, a schematic illustration of titania microballs formation with different exposed facets has been presented in Fig. 7. During an alcohotermal reaction (pure ethanol), initially equidimensional anatase nanocrystals precipitate (nucleate and grow) by consuming of the nanogel with a higher bulk energy (higher surface energy and higher solubility than anatase crystals), then anatase nanocrystals grow abruptly along [001] direction, driven in part by a relatively high surface energy of {001} surface and in part by a kinetic effect involving a cyclic generation of highly reactive adsorption sites. Subsequently, the growth stage involves an acceleration along [101] direction and a retardation along [001] direction to form the octahedral structure with length (the diameter along [001] direction) to diameter (the diameter along [101] direction) ratio of ca. 1.4 (the FE-SEM image in the left part of Fig. 7), which results from ca. 1.4 times larger surface energy of {001} than {101} facets [35]. With a decrease in ethanol/water ratio from 60:0 to 58:2 or 56:4, H-bonding, originated from water in {001} facets, might hinder the growth along [001], and thus exposing the thermodynamically unstable {001} facets. Therefore, the diameter along [001] direction becomes equal to that along [101] direction, and thus the truncated octahedron is formed (Fig. 4b, c). With a decrease in

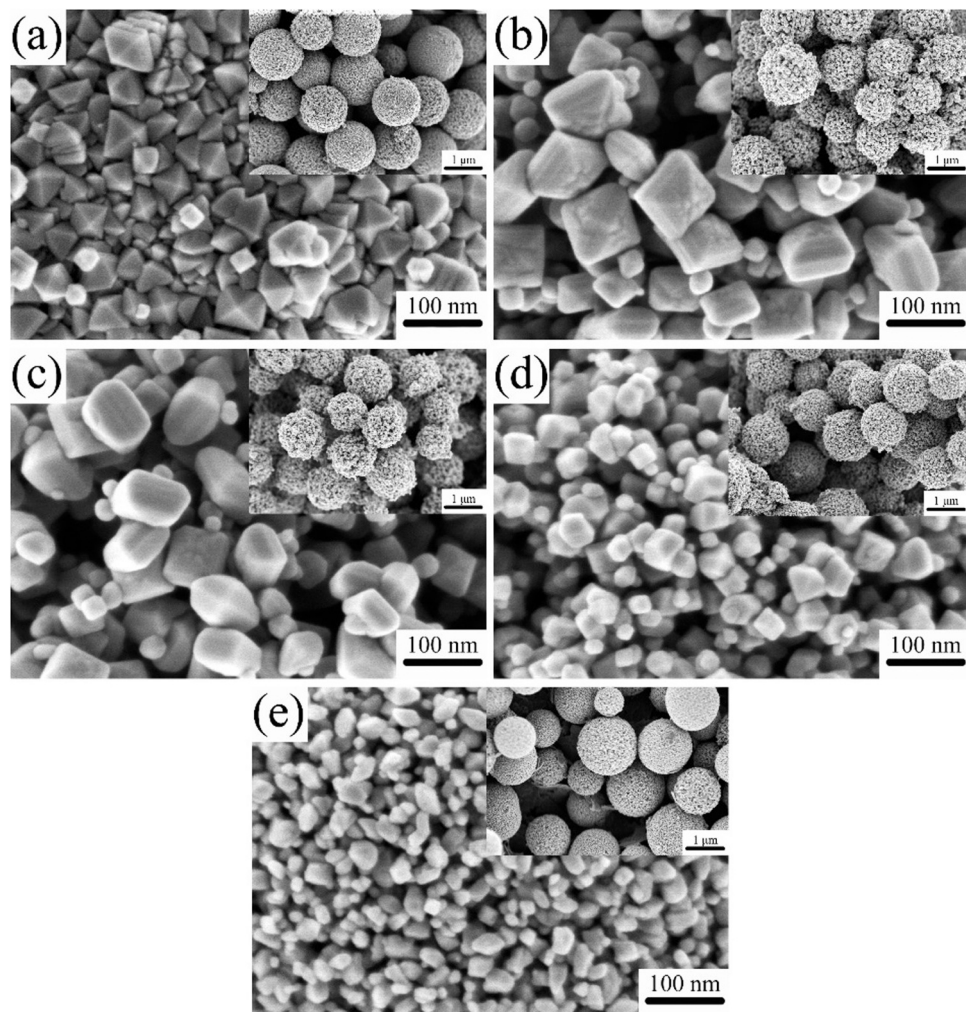


Fig. 4. FE-SEM images of the crystalline mesoporous microballs prepared during hydrothermal/alcohotermal treatment of S1 sample at 200 °C for 48 h with volume ratio of ethanol to water of: (a) 60:0, (b) 58:2, (c) 56:4, (d) 54:6 and (e) 0:60; Insets show the low-magnification images.

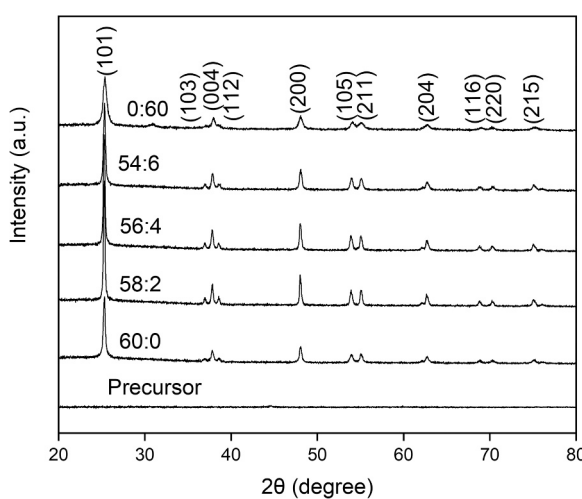


Fig. 5. XRD patterns of microballs built of amorphous (S1) and crystalline titania (anatase): prepared during hydrothermal/alcohotermal treatment with various volume ratios of ethanol to water.

ethanol/water ratio to 54:6, anatase crystals grow as truncated tetragonal bipyramids enwrapped with a large area of thermodynamically stable low-energy {101} facets and a small area of high-energy {001}

facets (the FE-SEM photograph in the right part of Fig. 7), which demonstrates that the ratio of ethanol to water has an important influence on the morphology of the mesoporous structure. The further decrease in ethanol/water ratio to 0:60 (pure water) results in a difficult control of the crystal growth (in an aqueous medium), due to high reactivity toward moisture of precursor microballs, which causes a coexistence of both octahedral and decahedral particles in the final product (Fig. 4e).

3.4. Photocatalytic activity under UV/vis irradiation

In order to evaluate the photocatalytic activity of obtained materials, four reaction systems have been examined. First, oxidative decomposition of MO has been investigated, and obtained data are shown in Fig. 8 (left). Indeed, crystalline samples (Octa and Deca) exhibit high photocatalytic activity, whereas amorphous titania decomposes dye hardly. Much higher activity of decahedral anatase than octahedral one has not been surprising since similar results have already been reported, e.g., for faceted anatase NPs with octahedron and decahedron shapes [14,15,18]. It has been proposed that the intrinsic separation of charge carriers in decahedral crystals, i.e., preferential migration of electrons and holes to {101} and {001} facets, respectively [33,34], is the main reason of its best performance. However, here additional tests have been performed for checking if and how the properties of titania influence the charge carriers' recombination/separation. For this purpose, the photoluminescence spectroscopy, photocurrent generation and

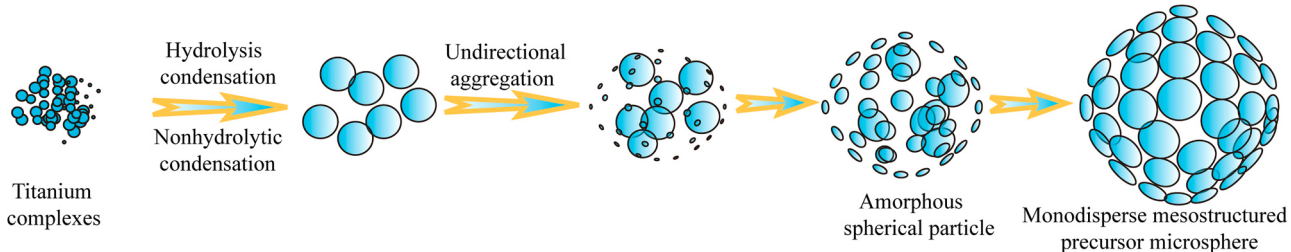


Fig. 6. Schematic representation on the formation mechanism of the mesoporous titania microballs.

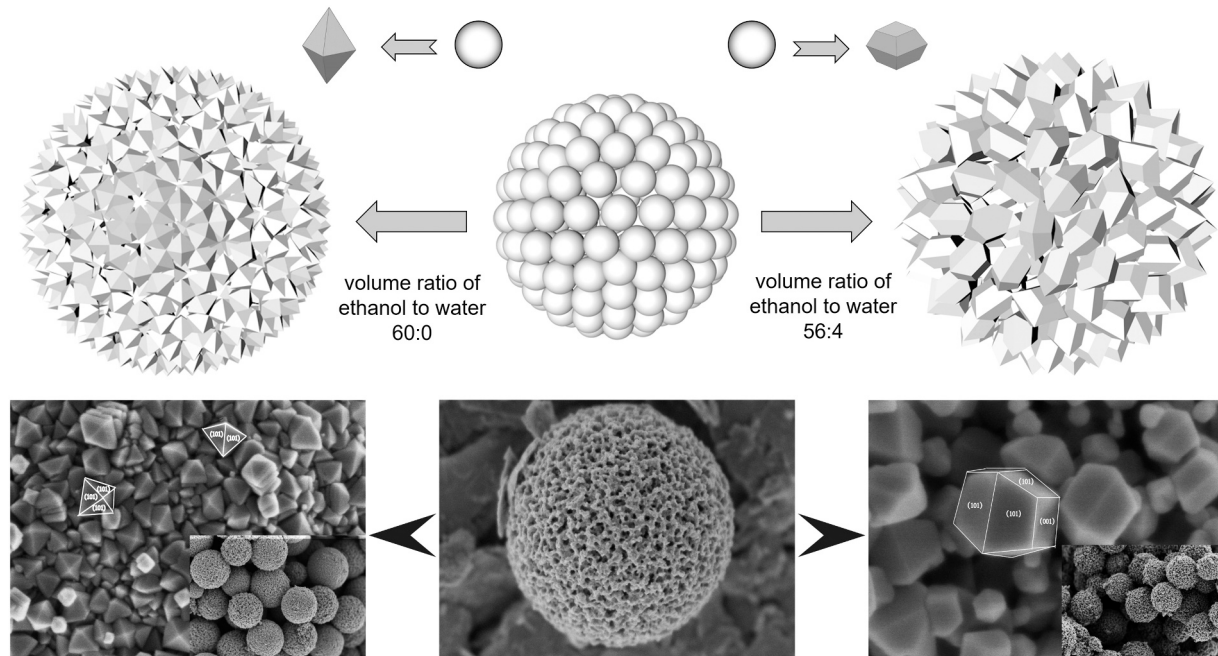


Fig. 7. (top) Schematic illustration on the formation of mesoporous microballs composed of faceted anatase nanocrystals with octahedron and decahedron morphology; (bottom) respective FE-SEM images.

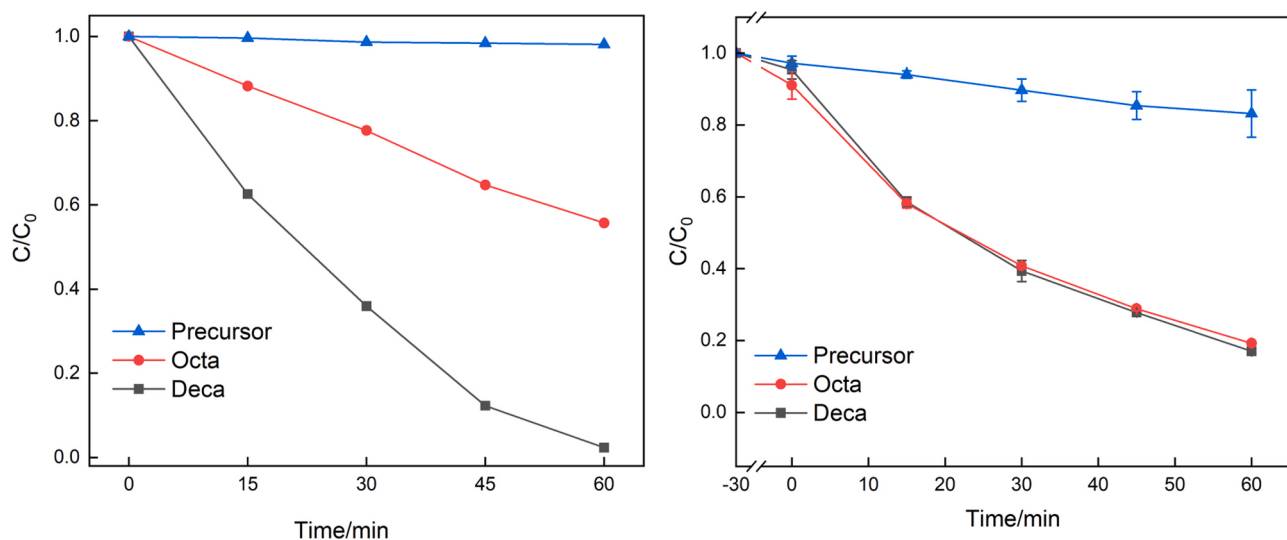


Fig. 8. Photocatalytic activity of mesoporous microspheres during oxidative decomposition of organic compounds: MO (left) and TC (right).

electrochemical impedance have been performed, and obtained data are shown in Fig. S2. Surprisingly, all tests indicate that octahedral titania, i.e., with only one type of facets {101}, should have the best performance,

i.e., the smallest photoluminescence peak, the highest photocurrent, and the smallest semicircle in the Nyquist plot, indicating the lowest charge carriers' recombination and the fastest electron migration. These results

showing a good performance of anatase bipyramids (octahedrons) correlate with other studies on octahedral anatase particles, indicating that the preferential formation of shallow rather than deep electron traps (ETs) allows the fast electrons' migration in these crystals (proven by a time-resolved microwave conductivity method and photoacoustic spectroscopy [15]). However, the fastest oxidation of MO (Fig. 8 (left)) on Deca with similar properties to Octa (even slightly worse specific surface area: 53.1, 41.9 and 89.1 m²/g for Octa, Deca and Precursor, respectively), could not be explained by the fastest charge carriers' separation and migration in these crystals (Fig. S2). Accordingly, another possibility has been considered, i.e., an ability to adsorbed water on the surface, which could result in more efficient formation of hydroxyl radicals, and thus efficient oxidative degradation of organic compounds, as already reported [35,36]. Indeed, the measurements of water contact angle (Fig. S3) confirms that Deca has much higher hydrophilic behavior than Octa and Precursor, i.e., 15° (classified as strong water wet), 51° (water wet) and 46° (water wet), respectively. Accordingly, its best performance should result from more efficient generation of hydroxyl radicals, e.g., adsorbed water might stabilize the photogenerated holes [35,36].

Although usually deposition of noble metals causes significant activity enhancement [35–37], here only slight improvement has been obtained in the platinum case, whereas even a decrease in activity has been observed after modification with gold and silver (Fig. S4). In the literature, similar examples could be found, suggesting that optimization of noble-metal content must be performed first [38–40]. It should be pointed out that too large metal content could result in the “inner-filter effect”, i.e., noble metals are blocking titania photoabsorption. Additionally, the deposition of noble metals on the surface of titania might disturb the reactants' adsorption. Moreover, especially in the present case, the mesopores might be plugged with NPs of noble metals. Accordingly, even though noble metals are usually recommended for hindering the charge carriers' recombination (working as a sink for electrons and Schottky barrier formation), they are not recommended in the case of oxidative degradation of MO on the mesoporous titania, composed of faceted anatase NPs. It might be concluded that the main function of noble metals, i.e., as a sink for electrons (to hinder their recombination with holes), is not so important in the case of faceted anatase samples (usually of very high activity) due to their intrinsic properties, i.e., the low-charge carriers' recombination (either by preferential existence of shallow rather than deep electron traps in octahedral anatase particles [15] or intrinsic separation of charge carriers in decahedral anatase particles [16]).

Additionally, the comparison between the photocatalytic activity of microballs and that by famous P25 (commonly used as a reference) has been performed, and obtained data are shown in Fig. S5. It has been found that similar activity is observed for gold-modified Deca and P25 samples, P25 is the most active among pristine and silver-modified samples, whereas platinum-modified Deca is the most active sample among all. Accordingly, it might be concluded that microballs are highly attractive, considering both their high activity and convenient size, allowing their easy recycling (in contrast to P25 with high costs of its separation after use).

Although MO is not considered as a good sensitizer [41], and the photocatalytic activity tests have been investigated under UV/vis (and thus mainly titania bandgap excitation is responsible for the overall effect), another organic compound (TC) has also been tested to prove that high photocatalytic activity originates from the properties of titania. The obtained data are shown in Fig. 8 (right). Indeed, crystalline microballs have proven high photocatalytic activity (similar to that by famous P25, Fig. S6) even for degradation of antibiotic. Interestingly, both crystalline samples exhibit similar activity, suggesting that hydrophilic behavior of Deca, and thus hydroxyl radicals as the main oxidative species are not the most crucial for this reaction.

Accordingly, the mechanism investigations have been performed, i.e., scavenger tests, and the obtained data are shown in Fig. 9. As

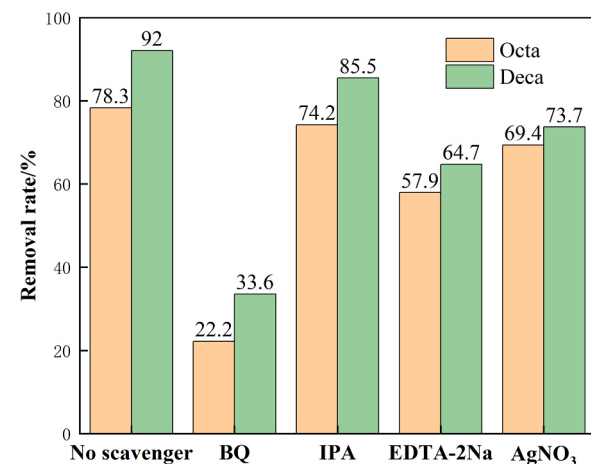


Fig. 9. Photocatalytic degradation of TC on titania microballs composed of octahedral and decahedral NPs in the presence of scavengers.

expected, superoxide anions (BQ as a scavenger) play the most significant role in TC degradation, confirming that charge carriers (direct redox reactions between TC and photogenerated electrons/holes) as well as hydroxyl radicals are not key reactants.

Following that, TC degradation on noble-metal-modified microballs has been conducted, and obtained data are shown in Fig. 10. Like MO degradation, only some platinum-containing crystalline samples show slight activity enhancement. However, in the case of amorphous titania, all metals have significant impact on the activity improvements. This is not surprising since the main feature of amorphous materials is the fast charge carriers' recombination, resulting from the large content of defects (e.g., deep electron traps [42]), and thus the presence of noble metals (electron traps) should hinder the e⁻/h⁺ recombination. Moreover, the versatility of Pt-modified decahedral-based microballs has been proven also for degradation of other pharmaceuticals (oxytetracycline hydrochloride, ciprofloxacin and norfloxacin), as shown in supplementary part (Fig. S7).

Next, photocatalytic activity in reduction-based reactions has been investigated. First, evolution of hydrogen (half reaction of water splitting) has been examined, and obtained data are shown in Fig. 11. It should be remembered that pristine titania is hardly active for hydrogen evolution (as confirmed in Fig. 11 (a); max evolution rate of H₂ reaching only ca. 22 μmol h⁻¹), and thus noble metals are necessary co-catalyst of this reaction. Indeed, significant activity increase has been observed for modified samples, especially those containing platinum, reaching even ca. 20 and 100 times' increase for Pt/Au-modified Octa and Deca (ca. 400 and 730 μmol h⁻¹, respectively). For mono-metallic samples, the activity increases in the following order: Ag < Au < Pt. Similar data have already been found in the literature [43–46], and explained by the highest work function of platinum. The greater the difference is between the work function of metal (4.26, 5.1 and 6.35 eV for Ag, Au and Pt, respectively [43]) and the electron affinity of titania (4.0 eV), the higher is Schottky barrier (the electronic barrier formed by the band alignment at the semiconductor-metal interface). Accordingly, the higher Schottky barriers means the faster scavenging of electrons by metals, resulting in the highest rate of hydrogen formation (on the surface of deposited metal). In the case of bimetallic modification, an obvious enhancement of activity has been observed by the platinum presence, and thus Pt/Au samples are characterized by the best performance. However, a negative impact by silver is probably caused by already mentioned the inner-filter effect (when too many NPs are deposited on the titania surface) and due to much lower activity of silver than platinum as a co-catalyst for hydrogen formation.

Considering the difference between titania samples, obviously, the amorphous titania exhibits the worst performance, especially in the case

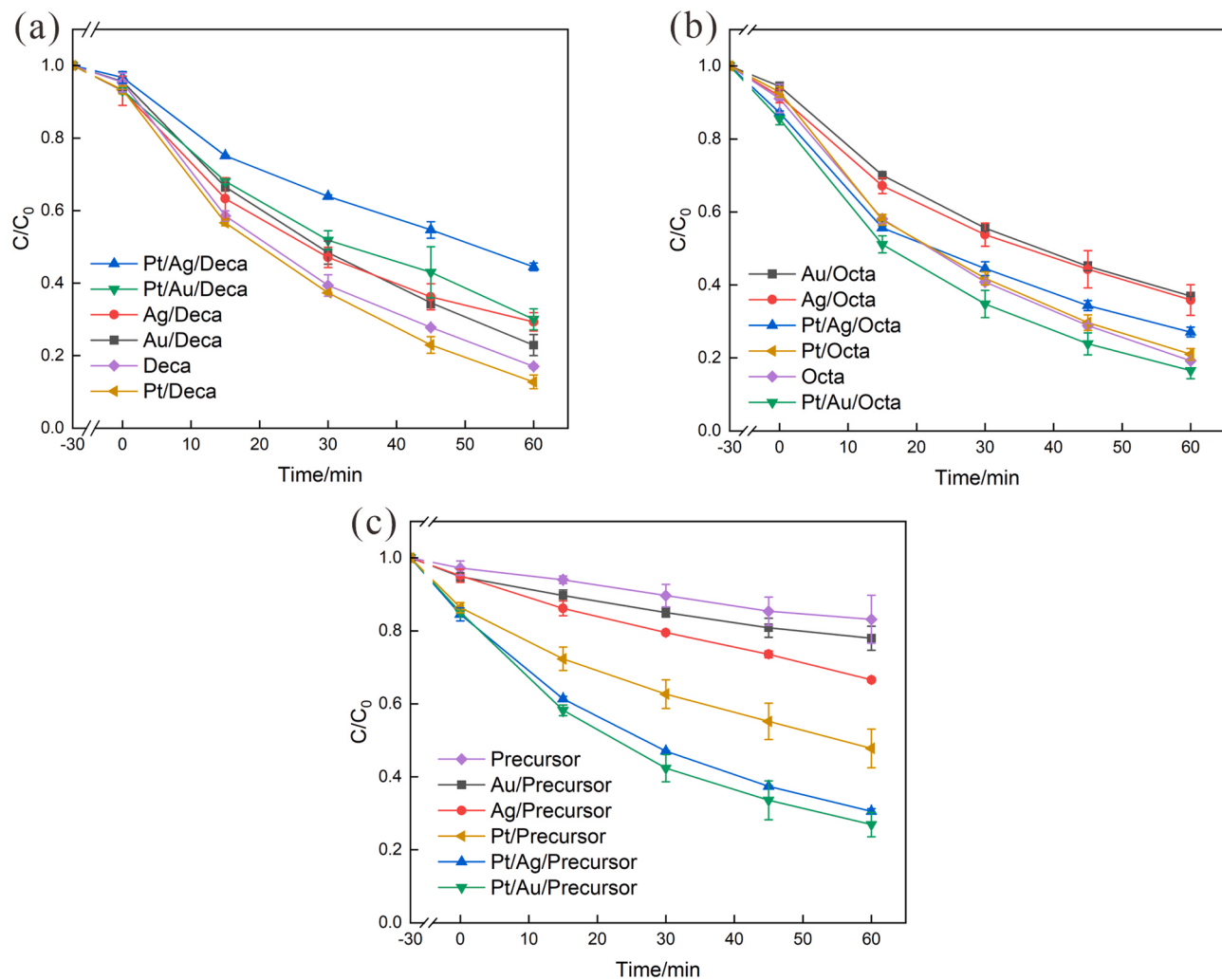


Fig. 10. Degradation of TC on pristine and noble-metal-modified microspheres composed of: (a) decahedral, (b) octahedral, and (c) amorphous titania.

of unmodified microballs (Fig. 11 (a)). However, deposition of metals increases its performance significantly, confirming the inhibition of charge carriers' recombination by deposited noble metals. For unmodified samples, Octa shows higher activity than Deca, corelating with reported data for faceted titania particles [18]. It has been proposed that though pristine titania is inactive for hydrogen evolution, slight activity could be observed, resulting from the presence of electron traps (ETs) with high energy (inside conduction band), and octahedral titania particles possess larger content of such defects [18]. Moreover, the higher mobility of electrons and the lower rate of charge carriers' recombination for Octa than Deca and Precursor (Fig. S2) correlate well with these activity data (in reduction reactions). In contrast, for all modified samples, Deca-based microballs exhibit the highest activities, even exceeding that by famous titania sample – P25 (commonly used as a reference due to exceptionally high activity for different reactions [47–49]), as shown in the supplementary file (Fig. S8). It is proposed that its special morphology, and thus selective reactions occurring on {101} and {001} facets, i.e., hydrogen formation (proton reduction) and oxidation of TEOA (used as a hole scavenger), respectively, is responsible for the high level of activity.

To confirm the reduction ability of noble-metal-modified microballs, carbon dioxide reduction has been investigated for the most active samples, i.e., modified with Pt/Au, and obtained data are shown in Fig. 12 and S9. Two main reduction products have been detected, i.e., methane (Fig. 12 (a)) and carbon monoxide (Fig. 12 (b)). Moreover, low content of ethane and ethene has also been formed (Fig. S10).

Additionally, hydrogen has also been evolved (Fig. 12 (d)), but at much slower rate than that during standard water reduction reaction (Fig. 11 (c)), which is reasonable, considering that water and carbon dioxide compete for photogenerated electrons.

Interestingly, octahedral-based microballs show much higher activity than decahedral ones, especially in the case of CO formation. It should be pointed out that for metal photodeposition on faceted titania, nanoparticles are mainly formed (respective metal cations are reduced first by photogenerated electrons) on {101} surface [50–52], which results from intrinsic charge carriers' separation inside titania crystals (electrons and holes migrate to {101} and {001} facets, respectively). Accordingly, in the case of decahedral-shaped titania, usually all noble metals are deposited preferably on {101} facet, keeping {001} empty [53,54], as also confirmed in this study (Fig. S11). Therefore, considering that noble metals, besides the inhibition of charge carriers' recombination, might enhance the adsorption and reduction of CO₂ molecules [55], it is concluded that CO₂ should be more efficiently adsorbed and reduced on {101} facet with Pt/Au deposits. Accordingly, the highest activity of Pt/Au/Octa with only {101} facet is thus reasonable. Interestingly, Pt/Au/Octa sample also shows the highest selectivity towards CO formation (ca. 65%). It should be remembered that in the case of CH₄ formation, the abundance of hydroxyl groups on the titania surface must be provided [56]. Here, all samples exhibit hydrophilic behavior, and thus high content of CH₄ is reasonable.

It should be underlined that high photocatalytic activity in CO₂ reduction on microballs might also be caused by their porous nature

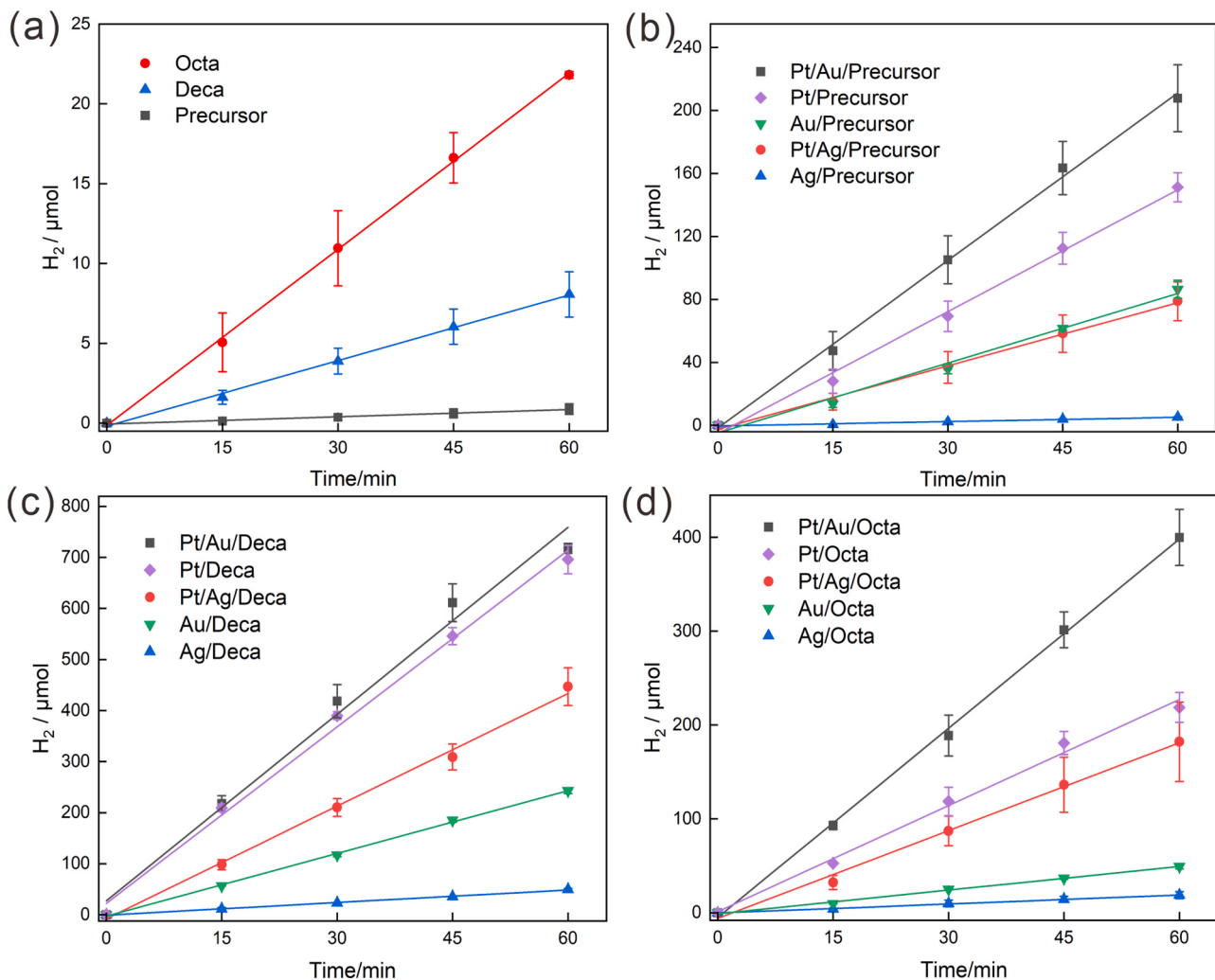


Fig. 11. Hydrogen evolution on pristine (a) and noble-metal-modified (b-d) microspheres composed of: (b) amorphous, (c) decahedral, and (d) octahedral titania.

[56]. It has already been reported that mesopores do not only facilitate the exposure of more catalytic active sites, but also boost the CO₂ adsorption/activation, and promote the mass and charge carrier transport [55].

3.5. Photocatalytic activity under vis irradiation

Photocatalytic activity under vis irradiation has been examined for noble-metal-modified samples, and the obtained data are shown in Fig. 13. It should be underlined that there is no hydrogen evolution on pristine samples (without noble metals). It is well known that titania (as also other wide-bandgap semiconductors) is inactive under vis irradiation. Accordingly, various modifications have been applied to shift its absorption towards vis range of solar radiation. Probably, one of the newest methods is to prepare plasmonic photocatalysts, i.e., to modify the surface of titania by deposits of noble metals. Although, such modification has been known for more than fifty years (started by Bard [57]), it was originally performed for other purposes (mainly to hinder the charge carriers' recombination), and the use of plasmonic feature for photocatalysis is still new, and not fully explored and understood (besides many fruitful papers [58–62], including also some reviews [63–66]). It should be noted that though plasmonic photocatalysts have shown vis activity, this activity is usually very low, resulting from the fast recombination of charge carriers. For example, in the case of charge-carrier-transfer mechanism, the “hot” (plasmonic) electrons might migrate from noble metals to the conduction band of titania, and

then to adsorbed molecules, but reverse transfer is highly competitive (NM → TiO₂ → NM [18]), considering the higher work function of these metal than an electron affinity of titania. Moreover, plasmonic photocatalysts are usually active in oxidative reactions, whereas negligible activity for reduction reactions has been reported [67]. This is reasonable, considering that hydrogen evolution takes mainly place on the deposits of metallic co-catalysts. Indeed, also in this study, though vis-response has been observed (Fig. 13), the level of activity is 2–3 orders in magnitude lower than that under UV irradiation (Fig. 11). Interestingly, bimetallic samples are more active than monometallic ones composing them (also different from UV performance), which should result from more efficient light harvesting ability (by two metals), as clearly observed by diffuse-reflectance spectra (Fig. S12). Moreover, the order of activity does not correlate with work function of metals (like under UV irradiation), but probably with plasmonic feature. For monometallic samples, microballs containing gold are the most active, whereas silver ones are the worst. In the literature, various contradictory data on the photocatalytic activity by different metals could be found [68,69]. Of course, broader plasmonic peak means more absorbed photons, and thus higher photocatalytic activity, as already proven for monometallic (samples containing noble-metal deposits of different sizes and shapes [59,70,71]) and some bimetallic materials (contrary results could be found, suggesting that despite more absorbed photons, the higher charge carriers' recombination could happen [72–74]). However, here, the deposited nanoparticles (NPs) of noble metals have similar sizes and shape (spherical). Moreover, the size of

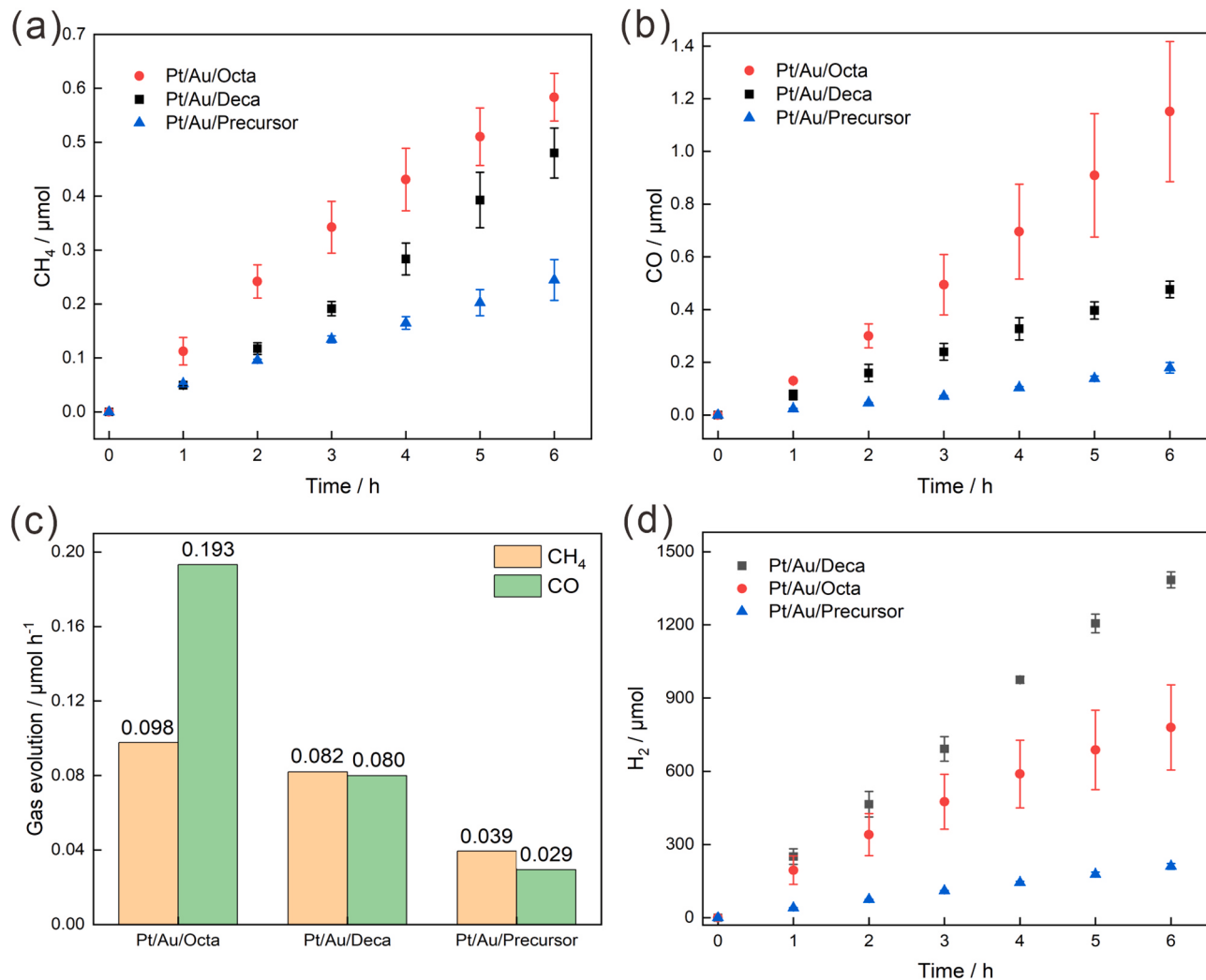


Fig. 12. Evolved gases (methane (a), carbon monoxide (b), both (c), and hydrogen (d)) during carbon dioxide reduction on Pt/Au-modified microspheres.

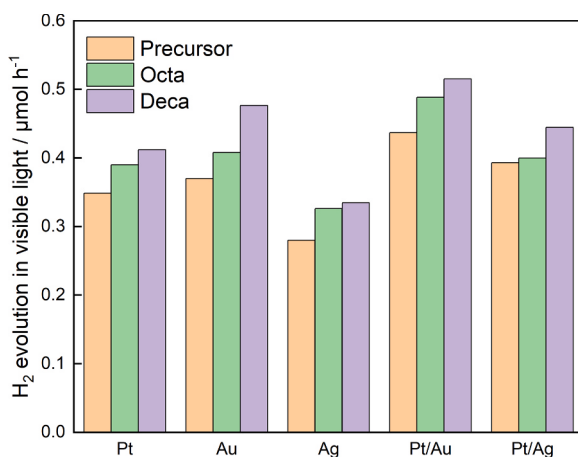


Fig. 13. Hydrogen evolution under vis irradiation on noble-metal-modified microspheres.

NPs does not differ significantly between noble metals (5–20 nm), as shown in Fig. S13. Of course, it is impossible to conclude unequivocally that gold is the best without the optimization study since the optimal amount of noble metal could depend on the metal type. Indeed, the previous study on gold-modified titania has shown that activity under

vis irradiation depends on the content (and thus properties: size and shape) of gold, which is directly influenced by titania properties (size and content of defects) [75]. However, due to impossibility to perform optimization studies (including three monometallic and two bimetallic samples for three types of microballs and five reaction systems) and based on the comparison between activity under UV and vis (Fig. 11 vs Fig. 14) as well as the previous experience, it is proposed here, that the type of noble metal is decisive for the performance under vis, and thus simulations of plasmonic properties have been examined, as shown in Fig. 14.

Indeed, gold-based sample is characterized by the strongest field enhancement. For a large micrometer-sized titania sphere, the main localization of light at visible wavelengths is inside it with a well-defined surface enhancement pattern of morphology dependent resonances (MDR). The MDRs are corresponding to standing circumferential surface wave, which cause a significant light enhancement at the wave crests. This global light distribution is not fundamentally changed when a micro-sphere is composed from nano-pyramids (data not shown here). As qualitatively expected, light field enhancement is locally increased at the sharpest edges of those nano-pyramids, however, the global pattern of light distribution is qualitatively similar to the microsphere case shown in Fig. 14.

The MDR caused light redistribution is also reflected in the scattering and absorbance cross-sections which have strongly oscillating spectral features. Once a metallic nano-sphere is added into light field on a

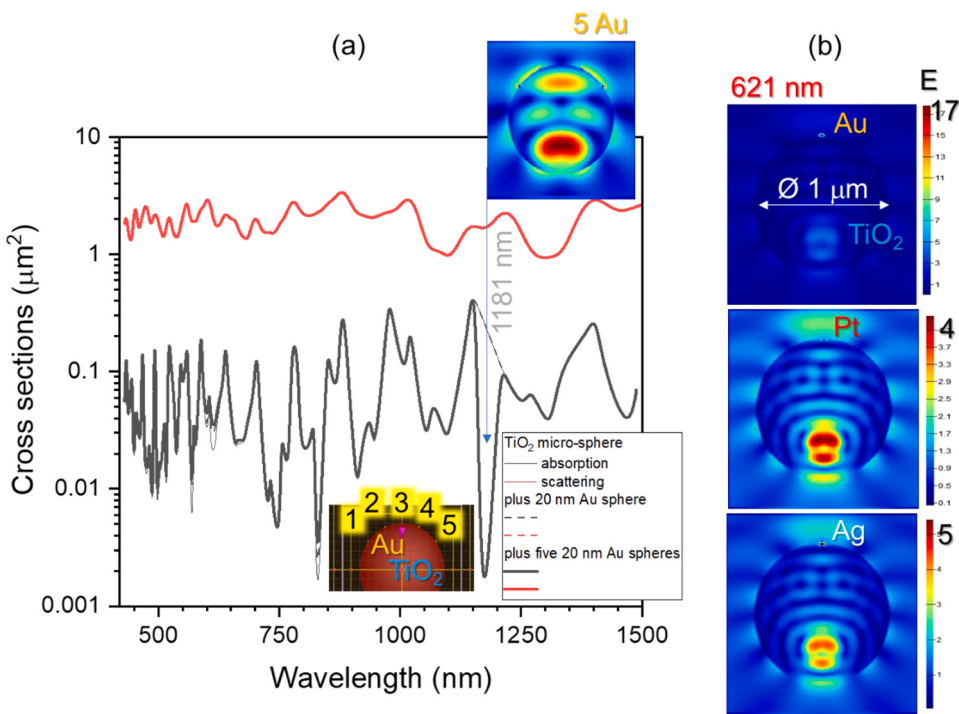


Fig. 14. Numerical modeling of light absorption and scattering from a 1-mm-diameter with 20-nm-diameter nanoparticles: (a) Cross-sections of absorption and scattering calculated with Lumerical (Ansys) using material database for wavelength specific complex refractive index ($n + ik$). (b) Central cross sections of metal decorated titania microparticle at 621 nm wavelength. The incident light has $E = 1$, and strong enhancement inside the titania microparticle as well as near the metal nanoparticles is evident. “5 Au” states for five 20-nm Au spheres.

surface of micro-sphere, the local enhancement takes place. This enhancement is material and size dependent and is recognizable on the global spectra of a titania micro-sphere (Fig. 14a). For red light (621 nm), gold NP causes the strongest localized enhancement as compared with the same sized 20-nm-diameter Pt and Ag nanospheres (Fig. 14b).

Nanoparticles of larger sizes scatter (reflection is part of scattering) more than absorb. At approximately 80–100 nm diameter nanospheres, scattering and absorption cross sections become comparable. This size dependence is highly important for various plasmonic applications.

4. Conclusions

Mesoporous anatase titania microballs with exposed facets could be efficiently prepared by simple and “green” method. It has been found that the tuning of synthesis conditions results in the preparation of microballs composed of different titania nanocrystals, i.e., octahedral- and decahedral-shaped NPs. Accordingly, these exposed facets are decisive for high photocatalytic response in different photocatalytic reactions.

It has been confirmed that decahedral-shaped, i.e., with highly energetic {001} facets, titania possesses much higher activity than other titania samples in oxidation reaction of organic dye, despite not the best properties of charge carriers’ separation and transfer, probably due to its higher ability of hydroxyl radicals’ formation, resulting from the most hydrophilic surface. Interestingly, octahedral-shaped anatase shows the best performance for reduction reactions (proton and carbon dioxide reduction), which correlates well with its photoelectrochemical properties.

Interestingly, the modification of crystalline (octahedral and decahedral) microballs with noble metals does not enhance photocatalytic activity significantly under UV/vis for oxidative reactions (even a decrease could be observed for some systems, probably due to the inner-filter effect). However, a significant activity enhancement is achieved

for amorphous titania, which is reasonable, considering that noble metals are excellent scavengers of photo-generated electrons, and thus hindering charge carriers’ recombination (very fast in the case of amorphous materials with large content of defects).

Moreover, the vis response via plasmonic photocatalysis is highly dependent on the type of noble metal. Here, despite similar size and shape, gold proves to be the best plasmonic “sensitizer”. It is proposed that in the comparison with silver and platinum, plasmon field is enhanced the strongest on gold deposits, as confirmed by FDTD simulations.

It is proposed that microballs composed of faceted nanoparticles are highly recommended for various photocatalytic applications, considering their high activity for both oxidation and reduction reactions and large size (helpful for possible recycling and commercialization).

CRediT authorship contribution statement

Kowalska Ewa Katarzyna: Project administration, Resources, Supervision, Writing – original draft, Writing – review & editing. **Juodkazis Saulius:** Data curation, Methodology, Writing – original draft. **Wu Limeng:** Investigation, Writing – original draft. **Wei Zhishun:** Conceptualization, Funding acquisition, Project administration, Writing – original draft, Writing – review & editing. **Yue Xin:** Investigation, Writing – original draft. **Li Zhenhao:** Investigation, Writing – original draft. **Mu Haoran:** Investigation, Visualization. **Janczarek Marcin:** Data curation, Writing – original draft. **Chang Ying:** Methodology, Validation, Writing – original draft, Resources.

Declaration of Competing Interest

The authors declare that they have no known competing financial interests or personal relationships that could have appeared to influence the work reported in this paper.

Data availability

Data will be made available on request.

Acknowledgment

This research was funded by National Natural Science Foundation of China (NSFC) (51802087), the Natural Science Foundation of the Hubei province of China (2019CFCB524), the Green Industry Leading Program of Hubei University of Technology (XJ2021002101). The project is co-financed by the Polish National Agency for Academic Exchange within Polish Returns Program (BPN/PPO/2021/1/00037) and the National Science Center (2022/01/1/ST4/00026).

Appendix A. Supporting information

Supplementary data associated with this article can be found in the online version at [doi:10.1016/j.apcatb.2023.123654](https://doi.org/10.1016/j.apcatb.2023.123654).

References

- [1] S. Yuan, Q. Sheng, J. Zhang, H. Yamashita, D. He, Synthesis of thermally stable mesoporous TiO₂ and investigation of its photocatalytic activity, *Microporous Mesoporous Mater.* 110 (2008) 501–507.
- [2] J. Tang, Y. Wu, E. McFarland, G. Stucky, Synthesis and photocatalytic properties of highly crystalline and ordered mesoporous TiO₂ thin films, *Chem. Commun.* 14 (2004) 1670–1671.
- [3] W. Ho, J. Yu, S. Lee, Synthesis of hierarchical nanoporous F-doped TiO₂ spheres with visible light photocatalytic activity, *Chem. Commun.* 10 (2006) 1115–1117.
- [4] Z. Xiong, H. Dou, J. Pan, J. Ma, C. Xu, X. Zhao, Synthesis of mesoporous anatase TiO₂ with a combined template method and photocatalysis, *CrystEngComm* 12 (2010) 3455–3457.
- [5] K. Hou, B. Tian, F. Li, Z. Bian, D. Zhao, C. Huang, Highly crystallized mesoporous TiO₂ films and their applications in dye sensitized solar cells, *J. Mater. Chem.* 15 (2005) 2414–2420.
- [6] J. Seifert, J. Feckl, D. Fattakhova-Rohlfing, Y. Liu, V. Kalousek, J. Rathousky, T. Bein, Ultrasmall titania nanocrystals and their direct assembly into mesoporous structures showing fast lithium insertion, *J. Am. Chem. Soc.* 132 (2010) 12605–12611.
- [7] P. Periyat, N. Leyland, D. McCormack, J. Colreavy, D. Corr, S. Pillai, Rapid microwave synthesis of mesoporous TiO₂ for electrochromic displays, *J. Mater. Chem.* 20 (2010) 3650–3655.
- [8] P. Araujo, V. Luca, P. Bozzano, H. Bianchi, G. Soler-Illia, M. Blesa, Aerosol-assisted production of mesoporous titania microspheres with enhanced photocatalytic activity: the basis of an improved process, *ACS Appl. Mater. Interfaces* 2 (2010) 1663–1673.
- [9] C. Tsung, J. Fan, N. Zheng, Q. Shi, A. Forman, J. Wang, G. Stucky, A general route to diverse mesoporous metal oxide submicrospheres with highly crystalline frameworks, *Angew. Chem. Int. Ed.* 47 (2008) 8682–8686.
- [10] O. Prieto-Mahaney, N. Murakami, R. Abe, B. Ohtani, Correlation between photocatalytic activities and structural and physical properties of titanium(IV) oxide powders, *Chem. Lett.* 38 (2009) 238–239.
- [11] A. Nitta, M. Tahase, M. Takashima, N. Murakami, B. Ohtani, A fingerprint of metal-oxide powders: energy-resolved distribution of electron traps, *Chem. Commun.* 52 (2016) 12096–12099.
- [12] K. Wang, M. Janczarek, Z. Wei, T. Raja-Mogan, M. Endo-Kimura, T. Khedr, B. Ohtani, E. Kowalska, Morphology- and crystalline composition-governed activity of titania-based photocatalysts: overview and perspective, *Catalysts* 9 (2019) 1054.
- [13] H. Yang, C. Sun, S. Qiao, J. Zou, G. Liu, S. Smith, H. Cheng, G. Lu, Anatase TiO₂ single crystals with a large percentage of reactive facets, *Nature* 453 (2008) 638–642.
- [14] M. Janczarek, E. Kowalska, B. Ohtani, Decahedral-shaped anatase titania photocatalyst particles: synthesis in a newly developed coaxial-flow gas-phase reactor, *Chem. Eng. J.* 289 (2016) 502–512.
- [15] Z. Wei, E. Kowalska, J. Verrett, C. Colbeau-Justin, H. Remita, B. Ohtani, Morphology-dependent photocatalytic activity of octahedral anatase particles prepared by ultrasonication-hydrothermal reaction of titanates, *Nanoscale* 7 (2015) 12392–12404.
- [16] T. Tachikawa, T. Majima, Photocatalytic oxidation surfaces on anatase TiO₂ crystals revealed by single-particle chemiluminescence imaging, *Chem. Commun.* 48 (2012) 3300.
- [17] T. Tachikawa, T. Ohsaka, Z. Bian, T. Majima, Single-molecule fluorescence detection of effective adsorption sites at the metal oxide–solution interface, *J. Phys. Chem. C* 117 (2013) 11219.
- [18] Z. Wei, M. Janczarek, M. Endo, K. Wang, A. Balcytis, A. Nitta, B. Ohtani, E. Kowalska, Noble metal-modified faceted anatase titania photocatalysts: octahedron versus decahedron, *Appl. Catal. B Environ.* 237 (2018) 574–587.
- [19] W. Ho, J. Yu, S. Lee, Synthesis of hierarchical nanoporous F-doped TiO₂ spheres with visible light photocatalytic activity, *Chem. Commun.* 10 (2006) 1115–1117.
- [20] J. Yu, Q. Xiang, J. Ran, S. Mann, One-step hydrothermal fabrication and photocatalytic activity of surface-fluorinated TiO₂ hollow microspheres and tabular anatase single microcrystals with high-energy facets, *CrystEngComm* 12 (2010) 872–879.
- [21] S. Liu, J. Yu, M. Jaroniec, Tunable photocatalytic selectivity of hollow TiO₂ microspheres composed of anatase polyhedra with exposed {101} facets, *J. Am. Chem. Soc.* 132 (2010) 11914–11916.
- [22] Z. Zheng, B. Huang, X. Qin, X. Zhang, Y. Dai, M. Jiang, P. Wang, Highly efficient photocatalyst: TiO₂ microspheres produced from TiO₂ nanosheets with a high percentage of reactive {001} facets, *Chem. -Eur. J.* 15 (2009) 12576–12579.
- [23] X. Cheng, W. Leng, D. Liu, Y. Xu, J. Zhang, C. Cao, Electrochemical preparation and characterization of surface-fluorinated TiO₂ nanoporous film and its enhanced photoelectrochemical and photocatalytic properties, *J. Phys. Chem. C* 112 (2008) 8725–8734.
- [24] J. Yu, J. Yu, M. Leung, W. Ho, B. Cheng, X. Zhao, J. Zhao, Effects of acidic and basic hydrolysis catalysts on the photocatalytic activity and microstructures of bimodal mesoporous titania, *J. Catal.* 217 (2003) 69–78.
- [25] B. Ohtani, Y. Ogawa, S. Nishimoto, Photocatalytic activity of amorphous–anatase mixture of titanium(IV) oxide particles suspended in aqueous solutions, *J. Phys. Chem. B* 101 (1997) 3746–3752.
- [26] Z. Wei, M. Endo-Kimura, K. Wang, C. Colbeau-Justin, E. Kowalska, Influence of semiconductor morphology on photocatalytic activity of plasmonic photocatalysts: titanate nanowires and octahedral anatase nanoparticles, *Nanomaterial* 9 (2019) 1447.
- [27] S. Yuan, X. Bao, M. Chen, X. Qin, X. Chen, J. Zhang, C. Zhang, Unravelling the pathway determining the CO₂ selectivity in photocatalytic toluene oxidation on TiO₂ with different particle size, *Chem. Eng. J.* 470 (2023) 144138.
- [28] C. Bianchi, S. Gatto, C. Pirola, A. Naldoni, A. Di Michele, G. Cerrato, V. Crocellà, V. Capucci, Photocatalytic degradation of acetone, acetaldehyde and toluene in gas-phase: Comparison between nano and micro-sized TiO₂, *Appl. Catal. B Environ.* 146 (2014) 123–130.
- [29] A. Mamaghani, F. Haghight, C. Lee, Role of titanium dioxide (TiO₂) structural design/morphology in photocatalytic air purification, *Appl. Catal. B Environ.* 269 (2020) 118735.
- [30] K. Devi, P. Goswami, H. Chaturvedi, Fabrication of nanocrystalline TiO₂ thin films using sol-gel spin coating technology and investigation of its structural, morphology and optical characteristics, *Appl. Surf. Sci.* 591 (2022) 153226.
- [31] F. Dufour, S. Pigeot-Remy, O. Durupthy, S. Cassaignon, V. Ruaux, S. Torelli, L. Mariey, F. Maugé, C. Chanéac, Morphological control of TiO₂ anatase nanoparticles: what is the good surface property to obtain efficient photocatalysts?, *Appl. Catal. B Environ.* 174 (2015) 350–360.
- [32] W. Ni, S. Wu, Q. Ren, Silanized TiO₂ nanoparticles and their application in toner as charge control agents: preparation and characterization, *Chem. Eng. J.* 214 (2013) 272–277.
- [33] M. Khalil, F. Naumi, U. Pratomo, T. Ivandini, G. Kadja, J. Mulyana, Coexposed TiO₂'s (001) and (101) facets in TiO₂/BiVO₄ photoanodes for an enhanced photocatalytic fuel cell, *Appl. Surf. Sci.* 542 (2021).
- [34] F. Zhu, J. Wen, H. Guo, J. An, G. Wang, G. Ma, Low-temperature catalytic performance improvement of Ru/TiO₂(001) for o-dichlorobenzene oxidation, *Chem. Eng. J.* 473 (2023) 145186.
- [35] L. Mino, A. Zecchina, G. Martra, A. Rossi, G. Spoto, A surface science approach to TiO₂ P25 photocatalysis: an in situ FTIR study of phenol photodegradation at controlled water coverages from sub-monolayer to multilayer, *Appl. Catal. B Environ.* 196 (2016) 135–141.
- [36] L. Mino, F. Pellegrino, S. Rades, J. Radnik, V. Hodoroaba, G. Spoto, V. Maurino, G. Martra, Beyond shape engineering of TiO₂ nanoparticles: post-synthesis treatment dependence of surface hydration, hydroxylation, lewis acidity and photocatalytic activity of TiO₂ anatase nanoparticles with dominant {001} or {101} facets, *ACS Appl. Nano Mater.* 1 (2018) 5355–5365, 9.
- [37] K. Vikrant, M. Chung, D. Boukhvalov, P. Heynderickx, K. Kim, S. Weon, A platinum ensemble catalyst for room-temperature removal of formaldehyde in the air, *Chem. Eng. J.* 475 (2023) 146007.
- [38] K. Wang, E. Kowalska, Property-governed performance of platinum-modified titania photocatalysts, *Front. Chem.* 10 (2022) 972494.
- [39] M. Senevirathna, P. Pitigala, K. Tennakone, High quantum efficiency Pt/TiO₂ catalyst for sacrificial water reduction, *Sol. Energy Mater. Sol. Cells* 90 (2006) 2918–2923.
- [40] K. Wang, Z. Wei, B. Ohtani, E. Kowalska, Interparticle electron transfer in methanol dehydrogenation on platinum-loaded titania particles prepared from P25, *Catal. Today* 303 (2018) 327–333.
- [41] H. Shi, M. Gondal, A. Al-Saadi, X. Chang, Visible-light-induced photodegradation enhancement of methyl orange over bismuth oxybromide through a semiconductor mediated process, *J. Adv. Oxid. Technol.* 18 (2015) 78–84.
- [42] M. Janczarek, M. Endo-Kimura, K. Wang, Z. Wei, M. Akanda, A. Markowska-Szczupak, B. Ohtani, E. Kowalska, Is black titania a promising photocatalyst?, *Catalysts* 12 (2022) 1320.
- [43] Z. Wei, M. Endo, K. Wang, E. Charbit, A. Markowska-Szczupak, B. Ohtani, E. Kowalska, Noble metal-modified octahedral anatase titania particles with enhanced activity for decomposition of chemical and microbiological pollutants, *Chem. Eng. J.* 318 (2017) 121–134.
- [44] L. Wu, X. Yue, Y. Chang, K. Wang, J. Zhang, J. Sun, Z. Wei, E. Kowalska, Photocatalytic degradation of tetracycline under visible light irradiation on BiVO₄ microballs modified with noble metals, *Catalysts* 12 (2022) 1293.
- [45] D. Masih, Y. Ma, S. Rohani, Graphitic C₃N₄ based noble-metal-free photocatalyst systems: a review, *Appl. Catal. B Environ.* 206 (2017) 556–588.

- [46] K. Ji, H. Dai, J. Deng, H. Zang, H. Arandiyani, S. Xie, H. Yang, 3D.O.M. BiVO₄, supported silver bromide and noble metals: high-performance photocatalysts for the visible-light-driven degradation of 4-chlorophenol, *Appl. Catal. B Environ.* 168–169 (2015) 274–282.
- [47] F. Amano, T. Yasumoto, O. Prieto-Mahaney, S. Uchida, T. Shibayama, Y. Terada, B. Ohtani, Highly active titania photocatalyst particles of controlled crystal phase, size, and polyhedral shapes, *Top. Catal.* 53 (2010) 455–461.
- [48] O. Prieto-Mahaney, N. Murakami, R. Abe, B. Ohtani, Correlation between photocatalytic activities and structural and physical properties of titanium(IV) oxide powders, *Chem. Lett.* 38 (2009) 238–239.
- [49] K. Wang, Z. Wei, C. Colbeau-Justin, P25 and its components-electronic properties and photocatalytic activities, *Surf. Interfaces* 31 (2022) 102057.
- [50] L. Puntscher, K. Daninger, M. Schmid, U. Diebold, G. Parkinson, A study of Pt, Rh, Ni and Ir dispersion on anatase TiO₂(101) and the role of water, *Electrochim. Acta* 449 (2023) 142190.
- [51] J. Khan, M. Sayed, N. Shah, S. Khan, Y. Zhang, G. Boczkaj, H. Khan, D. Dionysiou, Synthesis of eosin modified TiO₂ film with co-exposed {001} and {101} facets for photocatalytic degradation of para-aminobenzoic acid and solar H₂ production, *Appl. Catal. B Environ.* 265 (2020) 118557.
- [52] Y. Cao, Q. Li, C. Li, J. Li, J. Yang, Surface heterojunction between (001) and (101) facets of ultrafine anatase TiO₂ nanocrystals for highly efficient photoreduction CO₂ to CH₄, *Appl. Catal. B Environ.* 198 (2016) 378–388.
- [53] W. Wang, M. Gao, X. Zhang, M. Fujitsuka, T. Majima, H. Yu, One-step synthesis of nonstoichiometric TiO₂ with designed (101) facets for enhanced photocatalytic H₂ evolution, *Appl. Catal. B Environ.* 205 (2017) 165–172.
- [54] J. Zhang, L. Zhang, X. Ma, Z. Ji, A study of constructing heterojunction between two-dimensional transition metal sulfides (MoS₂ and WS₂) and (101), (001) faces of TiO₂, *Appl. Surf. Sci.* 430 (2018) 424–437.
- [55] M. Marszewski, S. Cao, J. Yu, M. Jaroniec, Semiconductor-based photocatalytic CO₂ conversion, *Mater. Horiz.* 2 (2015) 261–278.
- [56] J. Ran, M. Jaroniec, S. Qiao, Cocatalysts in semiconductor-based photocatalytic CO₂ reduction: achievements, challenges, and opportunities, *Adv. Mater.* 30 (2018) 1704649.
- [57] B. Kraeutler, A. Bard, Heterogeneous photocatalytic preparation of supported catalysts: photodeposition of platinum on TiO₂ powder and other substrates, *J. Am. Chem. Soc.* 100 (1978) 4317–4318.
- [58] Y. Tian, T. Tatsuma, Mechanisms and applications of plasmon-induced charge separation at TiO₂ films loaded with gold nanoparticles, *J. Am. Chem. Soc.* 127 (2005) 7632–7637.
- [59] E. Kowalska, O. Prieto Mahaney, R. Abe, B. Ohtani, Visible-light-induced photocatalysis through surface plasmon excitation of gold on titania surfaces, *Phys. Chem. Chem. Phys.* 12 (2010) 2344–2355.
- [60] Z. Bian, T. Tachikawa, P. Zhang, M. Fujitsuka, T. Majima, Au/TiO₂ superstructure-based plasmonic photocatalysts exhibiting efficient charge separation and unprecedented activity, *J. Am. Chem. Soc.* 136 (2014) 458–465.
- [61] A. Luna, E. Novoseltceva, E. Louran, P. Beaunier, E. Kowalska, B. Ohtani, M. Valenzuela, H. Remita, C. Colbeau-Justin, Synergetic effect of Ni and Au nanoparticles synthesized on titania particles for efficient photocatalytic hydrogen production, *Appl. Catal. B Environ.* 191 (2016) 18–28.
- [62] P. DeSario, J. Pietron, T. Brintlinger, M. McEntee, J. Parker, O. Baturina, R. Stroud, D. Rolison, Oxidation-stable plasmonic copper nanoparticles in photocatalytic TiO₂ nanoarchitectures, *Nanoscale* 9 (2017) 11720–11729.
- [63] K. Ueno, H. Misawa, Surface plasmon-enhanced photochemical reactions, *J. Photochem. Photobiol. C* 15 (2013) 31–52.
- [64] S. Verbruggen, TiO₂ photocatalysis for the degradation of pollutants in gas phase: from morphological design to plasmonic enhancement, *J. Photochem. Photobiol. C* 24 (2015) 64–82.
- [65] M. Endo-Kimura, B. Karabiyik, K. Wang, Z. Wei, B. Ohtani, A. Markowska-Szczupak, E. Kowalska, Vis-responsive copper-modified titania for decomposition of organic compounds and microorganisms, *Catalysts* 10 (2020) 1194.
- [66] K. Christoforidis, P. Fornasiero, Photocatalytic hydrogen production: a rift into the future energy supply, *ChemCatChem* 9 (2017) 1523–1544.
- [67] M. Méndez-Medrano, E. Kowalska, A. Lehoux, A. Herissan, B. Ohtani, S. Rau, C. Colbeau-Justin, J. Rodríguez-López, H. Remita, Surface modification of TiO₂ with Au nanoclusters for efficient water treatment and hydrogen generation under visible light, *J. Phys. Chem. C* 120 (2016) 25010–25022.
- [68] E. Kowalska, K. Yoshiiri, Z. Wei, S. Zheng, E. Kastl, H. Remita, B. Ohtani, S. Rau, Hybrid photocatalysts composed of titania modified with plasmonic nanoparticles and ruthenium complexes for decomposition of organic compounds, *Appl. Catal. B Environ.* 178 (2015) 133–143.
- [69] Z. Wei, M. Janczarek, K. Wang, S. Zheng, E. Kowalska, Morphology-governed performance of plasmonic photocatalysts, *Catalysts* 10 (2020) 1070.
- [70] E. Kowalska, R. Abe, B. Ohtani, Visible light-induced photocatalytic reaction of gold-modified titanium(IV) oxide particles: action spectrum analysis, *Chem. Commun.* 2 (2009) 241–243.
- [71] S. Verbruggen, M. Keulemans, M. Filippousi, Plasmonic gold–silver alloy on TiO₂ photocatalysts with tunable visible light activity, *Appl. Catal. B Environ.* 156 (2014) 116–121.
- [72] M. Li, X. Jiang, J. Liu, Q. Liu, N. Lv, N. Qi, Z. Chen, A flower-like Co/Ni bimetallic metal-organic framework based electrode material with superior performance in supercapacitors, *J. Alloy. Compd.* 930 (2023) 167354.
- [73] U. Caudillo-Flores, M. Muñoz-Batista, M. Fernández-García, A. Kubacka, Bimetallic Pt-Pd co-catalyst Nb-doped TiO₂ materials for H₂ photo-production under UV and visible light illumination, *Appl. Catal. B Environ.* 238 (2018) 533–545.
- [74] P. Verma, Y. Kuwahara, K. Mori, H. Yamashita, Pd/Ag and Pd/Au bimetallic nanocatalysts on mesoporous silica for plasmon-mediated enhanced catalytic activity under visible light irradiation, *J. Mater. Chem. A* 4 (2016) 10142–10150.
- [75] E. Kowalska, S. Rau, B. Ohtani, Plasmonic titania photocatalysts active under UV and visible-light irradiation: influence of gold amount, size, and shape, *J. Nanotechnol.* (2012) 361853.